Int J Clin Exp Pathol 2025;18(4):148-165
www.ijcep.com /ISSN:1936-2625/IJCEP0162524

Original Article

Predictive model for prognosis, immune microenvironment and drug sensitivity of colon carcinoma based on cuproptosis-related genes

Bo Zhao*, Wenqi Lu*, Yongjun Chen*, Xiaoyong Cai

*Department of General Surgery, The Second Affiliated Hospital of Guangxi Medical University, Nanning 530021, Guangxi Zhuang Autonomous Region, The People's Republic of China. *Equal contributors.*

Received December 7, 2024; Accepted March 8, 2025; Epub April 15, 2025; Published April 30, 2025

Abstract: Background: Colon cancer is a major cause of morbidity and mortality worldwide. Copper-induced cell death, known as cuproptosis, is a form of apoptosis that has been extensively studied in human diseases and is widely associated with tumor progression, prognosis, and immune response. However, the role of cuproptosis-related genes (CRGs) in the tumor microenvironment (TME) of colon cancer remains unclear. Objective: This study aims to explore the role of cuproptosis-related long non-coding RNAs (lncRNAs) in predicting the prognosis of colon cancer and to establish a risk prediction model based on these lncRNAs to guide clinical decisions and improve patient outcomes. Methods: A total of 19 cuproptosis-related genes were collected, and 1330 lncRNAs associated with cuproptosis were identified. Seven cuproptosis-related lncRNAs with prognostic value were selected from The Cancer Genome Atlas (TCGA) database. Using R software (version 4.1.0), the expression levels of the 19 genes were extracted, and the subjects were divided into high- and low-risk subgroups. A risk score model was developed based on cuproptosis-related genes and the seven co-expressed lncRNAs. The dataset was randomly split into a training set and a validation set. Analysis of clinicopathologic features, TME infiltration, and mutations was conducted, and nomogram predictions were validated using calibration plots to assess the predictive accuracy of the model. Results: The high-risk group had significantly shorter overall survival compared to the low-risk group ($P<0.001$), and the risk score was an independent prognostic factor ($P<0.001$). In the training set, the AUC values at 1, 3, and 5 years were 0.666, 0.621, and 0.669, respectively. Furthermore, low-risk patients had a higher survival rate. The genetic markers also correlated with tumor immune cell infiltration, clinical features, and prognosis. Conclusion: This study established a novel method based on cuproptosis-related lncRNAs to predict the prognosis of colon cancer. The model has potential clinical applications in identifying patients sensitive to immunotherapy and antitumor treatments, thereby enhancing precision treatment strategies for colon cancer.

Keywords: Cuproptosis, LncRNA prognostic model, colon carcinoma, tumor microenvironment

Introduction

Colorectal cancer (CRC) is the 3rd most common cancer worldwide and is a leading cause of cancer-related mortality [1]. Tumor cell activity, proliferation, and intercellular communication are influenced by not only the tumor cells themselves but also the entire tumor microenvironment (TME), which includes stromal cells, immune cells, extracellular matrix molecules, cytokines, and tumor-associated macrophages, all playing crucial roles in tumor growth and metastasis [2-5]. Among these, the tumor immune microenvironment (TIME) has emerged as a critical determinant in CRC progression, influencing both carcinogenesis and metastasis [6, 7].

Copper, an essential trace element, plays a vital role in several cellular processes, including mitochondrial respiration, oxidative resistance, and detoxification. Imbalances in copper levels have been linked to various diseases, including cancer. Recent studies suggest that copper may promote tumor progression by regulating processes like cell proliferation, angiogenesis, and metastasis [8-11]. A newly identified form of programmed cell death, known as cuproptosis, is induced by copper binding to lipoylated components of the tricarboxylic acid (TCA)

https://doi.org/10.62347/FEEF1483

cycle, leading to proteotoxicity, mitochondrial dysfunction, and cell death. This mechanism may offer novel anti-tumor strategies by generating reactive oxygen species (ROS) and activating apoptotic signaling pathways [12, 13]. Research into cuproptosis-related genes (CRGs) is still in its early stages, but these genes have garnered attention for their potential as biomarkers to predict cancer prognosis and therapy responses, particularly with regard to immunotherapy and targeted treatments [14]. While studies on cuproptosis mechanisms and their implications in the TME are still in early stages, evidence is emerging that CRGs could be used as biomarkers to predict cancer prognosis and response to therapy. However, more research is needed to fully understand the clinical application of CRGs in cancer treatment, particularly in terms of immunotherapy and targeted therapies.

Long noncoding RNAs (lncRNAs), which are non-coding transcripts over 200 nucleotides, have emerged as key regulators in cancer biology [15]. These molecules influence gene expression, translation, histone modification, and other post-transcriptional processes [16]. In CRC, lncRNAs have been shown to participate in tumor progression, immune evasion, and resistance to therapy. Recent evidence suggests that lncRNAs may modulate metabolic activities within the TME, influencing tumor survival and proliferation [17-19]. The interaction between CRGs and lncRNAs represents a promising area of research, that may lead to improved prognostic tools and therapeutic strategies for CRC.

Materials and methods

Data source and preprocessing

We generated RNA sequencing data (RNA-seq) from 480 colon adenocarcinoma (COAD) samples and 41 normal tissue samples from colon cancer patients using the TCGA database (https://portal.gdc.cancer.gov/), released on March 15, 2022. All samples were directly obtained from patients and included survival information, with mRNA expression data in Fragments Per Kilobase Million (FPKM) format. Clinical data, including age, sex, staging, and race/ethnicity, were collected from the TCGA data portal. Additionally, somatic mutation data from whole exome/genome sequencing (WXS/WGS) were retrieved from the GDC TCGA-COAD project on the UCSC Xena server [20]. The MuTect2 algorithm was used to identify high-confidence somatic variants and detect additional germline mutations [21]. The R package "mafTools" was used to plot Oncoplots in descending order of mutations [22], and the data were analyzed using R software (version 4.1.0) and Strawberry Perl.

Samples were included in the study if they were classified as colon adenocarcinoma (COAD) and contained complete clinical data (including survival information, age, sex, cancer staging, and race/ethnicity). Only samples with mRNA expression data in FPKM format and reliable somatic mutation data from WXS/WGS were considered. Exclusion criteria included samples that did not meet these requirements, such as those lacking sufficient clinical data, incomplete or low-quality mRNA expression data, or those without corresponding normal tissue for comparison. Additionally, samples without reliable somatic mutation data or those not classified as COAD were excluded.

Detecting the expression of Cuproptosis Related Genes (CRGs) and extraction of cuproptosis-related lncRNAs in colon cancer

To identify lncRNAs or to separate the non-coding and coding sections of transcriptome, Strawberry, for transcript reconstruction and quantification from RNA-Seq data was used. The expression level of cuproptosis-related lncRNAs were found by Cox regression analysis and Lasso regression. R software (v4.1.0) was used to extract gene expression data for 19 cuproptosis-related genes. To estimate the correlation coefficient and associated *p*-value (along with the confidence interval), we set up CorFilter and pvalueFilter at value of 0.4 and 0.001, respectively. The expression files of cuproptosis-related lncRNAs were downloaded from TCGA and the data were processed. Finally, 1330 lncRNAs associated with cuproptosis were identified by co-expression analysis and organized into an expression matrix, which was merged with survival information. Furthermore, the survival R package with pFilter = 0.01 was used for univariate Cox regression analysis to screen out 13 prognostic lncRNAs, and the corresponding forest map was drawn. The limma package, a commonly used R package, was used to analyze the differential expression

of lncRNAs related to prognosis between tumor and normal samples (*P<0.05, **P<0.01, ***P<0.001).

Gene network and enrichment analysis of CRGs

A gene network analysis was performed using GENEMANI to check possible interactions of cuproptosis-related genes [23]. In our study, R package "clusterProfiler" Gene Ontology (GO) and Kyoto Encyclopedia of Genes, and Genomes (KEGG) were used to analyze potential interactions between these genes as well as gene enrichment [24]. The Benjamini-Hochberg method was used for multiple corrections to obtain the false discovery rate (FDR) <0.05 considered as significant.

Construction and validation of cuproptosis-related lncRNAs prognostic model

We divided the samples randomly into training and test groups in a 1:1 ratio using the R package cart. Then, the smaller penalty term (i.e. the value of lambda (λ)), was chosen by cross-validation. The optimal model for prediction performance was then selected using the Glmnet R package, which was built based on the 7 lncRNAs. The risk score was calculated through the following formula:

$$Risk\ score = \sum_{i=1}^{n} Coef_i * x_i$$

Where Coef-i is the corresponding coefficient and *X*-i is the expression level of each prognostic lncRNAs, respectively. Patients were divided into high- and low-risk groups using the risk score based on this model. R Package survival, survminer, and timeROC were used for survival analysis and model evaluation as well as for the corresponding K-M survival curves and 1-, 3-, and 5-year ROC curves, which were performed on the training and test sets.

For this study, the number of groups was set as 1. The data were randomly divided into groups to construct a test model following performance of univariate Cox analysis in order to obtain meaningful lncRNAs by comparing the survival time and survival status of each sample. The LASSO regression model analysis was then carried out by single factor meaningful expression files following the point with the minimum error by cross-validation. At the end, the Cox model was constructed by the number of lncRNAs screened by LASSO regression.

We then constructed risk scores by using regression coefficients of the identified CRGs for the prognostic markers of OS and PFS. We divided patients into high- and low-risk groups based on the median risk score. Kaplan-Meier survival curves were drawn using R package "ggsurvplot" to compare OS or PFS between high- and low-risk groups. The R package "survivalROC" was used to calculate a receiver operating characteristic (ROC) curve to represent the predictive ability. Furthermore, we examined possible differences between subgroups stratified by age, gender, and tumor stage. The R package "regplot" was used to construct an enhanced regression nomogram of CRG score and other clinical covariates in patients with colon cancer. The calibration curves for CRGs scores and other clinical covariates in patients with colon cancer were computed using 1000 bootstrapping to evaluate of the performance the predicted bias-corrected estimates in comparison to the observed values analyzed using the R package "rms".

Colon cancer correlation with immune infiltration and drug sensitivity

The independent predictive value of the model and its applicability to various clinicopathologic characteristics of the cohort were studied in correspondence to the correlation of risk score with clinicopathologic factors and antitumor drug sensitivity, in high- and low-risk subgroups. We used the limma and ggpubr packages to query whether there were differences in risk score among different age groups and tumor stages as well as whether there was differential expression of the 7 prognostic lncRNAs between high-risk and low-risk subgroups. The limma, ggplot2, ggpubr, and ggExtra packages were used to detect a correlation between immune cell infiltration and risk score following instruction in the Tumor Immune Estimation Resource website (TIMER: https://cistrome.shinyapps.io/timer/) [25]. We investigated five copper-death genes that are co-expressed with lnc RNAs following investigation of their relationship with six immune cell types (i.e.; CD4+ T cells, CD8+ T cells, B cells, neutrophils, dendritic cells, and macrophages).

Also, pRRophetic package was used to predict the IC_{50} of an antitumor drug to identify a more effective subset of drug treatments where a lower IC_{50} indicates a higher sensitivity to the drug.

Statistical analysis

The R survival package was used for survival analysis. The survival rate of each group was tested by log-rank test hypothesis. The Kruskal-Wallis test was used to compare two or more groups of data using the Wilcoxon test. The Kaplan-Meier method was used to draw the survival curve of patients. The Chi-square test was used to analyze the frequency of colon cancer mutations, and Spearman analysis was used to calculate the correlation coefficient. R version 4.1.0 was used for all statistical analyses ($P<0.05$ was considered significant).

Results

Acquisition of genetic alterations of cuproptosis-related lncRNAs in colon caner

We downloaded transcriptome data of colon cancer from the TCGA database and from that, an mRNA expression matrix was divided into two parts, i.e.; mRNA and lncRNA following extraction of the expression of 19 Cuproptosis-Related genes from the mRNA expression matrix. The co-expression analysis yielded 1330 lncRNAs related to Cuproptosis. The Sankey map was drawn by R package "ggplot2" and "ggalluvi1" to determine the co-expression relationship between cuproptosis gene and related lncRNAs (**Figure 1**). The expression level of lncRNA in the risk model was extracted by reading expression files of cuproptosis-related lncRNA and processing the data.

Prognosis-related lncRNAs in colon cancer were screened by univariate Cox regression analysis and prognostic signature of cuproptosis-related genes

A total of 1330 lncRNAs associated with cuproptosis were extracted for univariate Cox regression analysis, following the univariate Cox significance filter standard set at 0.05 (coxPfilter0.05). Thirteen lncRNAs with prognostic significance were identified in which each one was labeled with pro-oncogenes (HR> 1, EIF1AX-AS1, AP002449.1, AC069222.1, AL138921.1, AC048344.4, AC090517.2, THCAT158, AC025171.4, MCCC1-AS1, ALMS1-IT1, AC012313.5, AC064836.3, AC010463.3) ($P< 0.01$) (**Figure 1D**). Differential analysis showed that the expression of each lncRNA for tumor specimens was significantly different in comparison to normal specimens. The number of groups was set to 1, and the data were randomly divided into groups to construct a test model following by univariate Cox analysis in order to obtain meaningful lncRNAs by comparing the survival time and survival status of each sample. The LASSO regression model was carried out by single factor meaningful expression files, where the point with the minimum error was found by cross-validation. The Cox model was the constructed by the number of lncRNAs screened by LASSO regression. According to the overall risk curve, we plotted the median risk values of the training and test groups, respectively. We found that the risk of death significantly increased with an increase of risk score. According to the risk heat map, we also intuitively found that the cuproptosis co-expressed lncRNAs such as: AC048344.4, AC090517.2, THCAT158, AC025171.4, and McCc1-as1. High level expression of ALMS1-IT1 lncRNA showed that these 5 lncRNAs correlated with high risk of copper mortality. In contrast, the expressions of EIF1AX-AS1 and AC012313.5 decreased along with an increase in risk score. This clearly showed that they were lncRNAs that correlated with low risk of cuproptosis (**Figure 2**).

Principal component analysis

Through principal component analysis, we were able to guide the lncRNAs involved in the model construction in order to distinguish colon cancer patients in high- and low-risk groups. They were divided as Cuproptosis-Related genes, Cuproptosis-Related lncRNAs, all gene sets, and model lncRNAs, respectively. Principal component analysis demonstrated a distinction between high- and low-risk lncRNAs. Also, lncRNA participating in the model construction could distinguish patients in both high- and low-risk groups.

Construction and validation of a risk predictive model

Initially, univariate Cox regression analysis was performed on 1330 lncRNAs associated with cuproptosis, and 7 lncRNAs were found to be

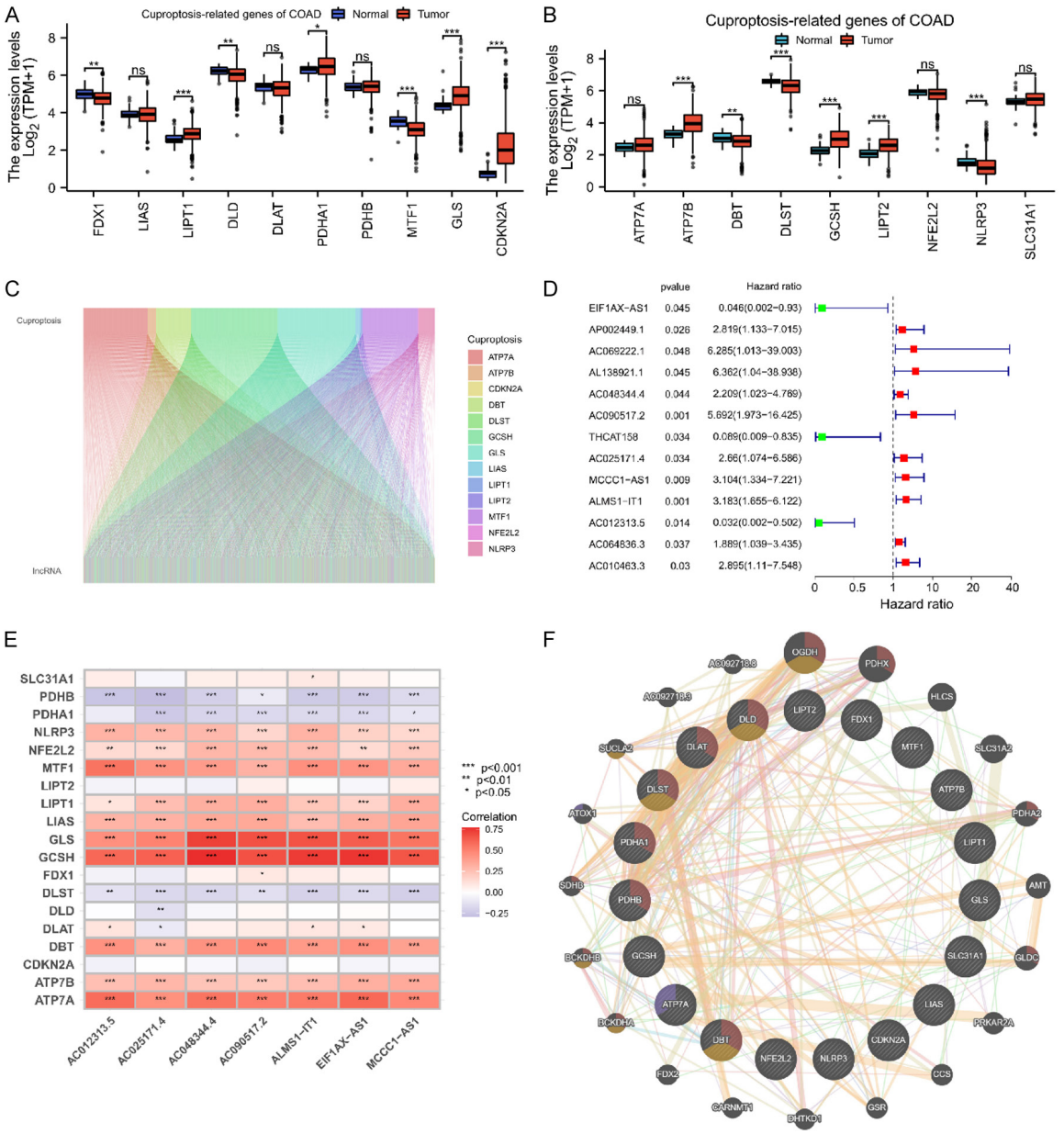

Figure 1. Differential expression and genetic alterations of cuproptosis-related lncRNAs in colon cancer patients: (A, B) Differential expression of copper death-related genes in colon cancer patients, (C) Sankey diagram of cuproptosis-related lncRNAs in colon cancer, (D) Univariate forest map of lncRNA for cuproptosis-related lncRNAs in colon cancer, (E) Heat map of cuproptosis-related lncRNAs co-expression in colon cancer, (F) Protein-Protein Interaction of cuproptosis-related genes.

significantly correlated with OS. Also, we performed Lasso regression analysis on 7 lncRNAs and a risk prognostic model was built. After collecting data and sampling where needed, the next step was to split data into training and validation sets with equal numbers according to one random cycle. **Figure 3** shows the risk scores, survival status, and expression of seven prognostic lncRNAs in two groups of samples. The risk score equation based on the model was: EIF1AX-AS1, AC048344.4, AC090517.2, AC025171.4, McCc1-as1, ALMS1-IT1, and AC012313.5. The K-M survival curves of the training and validation sets showed that the survival prognoses of high- and low-risk groups were significantly different, which was determined by the median risk score (the high-risk group had worse OS). Moreover, the overall

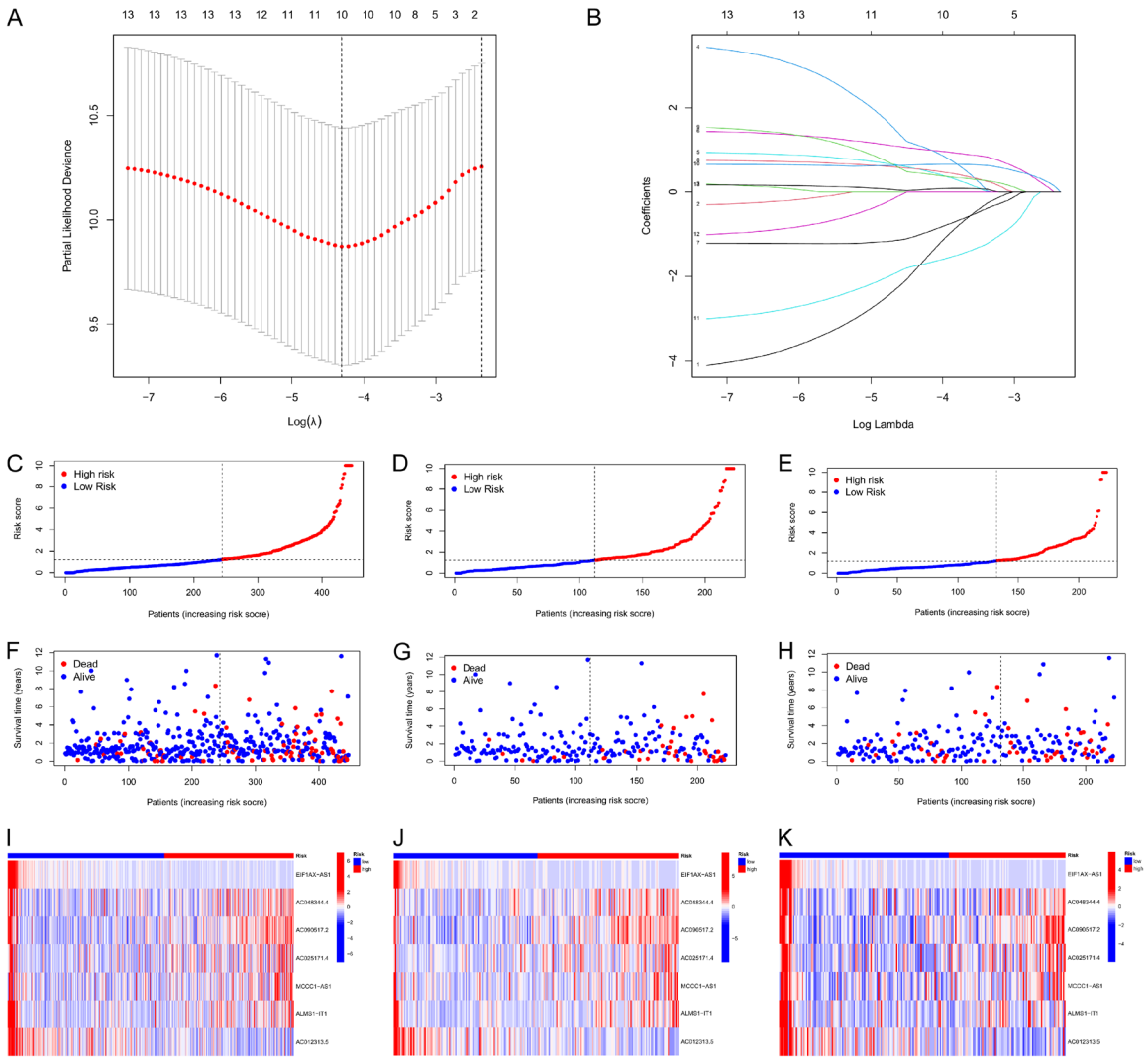

Figure 2. Construction of a prognosis risk prediction model: (A, B) The least absolute shrinkage and selection operator (LASSO) regression was performed with the minimum criteria, (C-E) Exhibition of Cuproptosis-Related lncRNAs prediction model based on risk score of the training, test, and entire sets, respectively, (F-H) Survival status of the high and low risk group between the high-and low-risk group in the training, test, and entire sets, respectively, (I-K) cuproptosis-related lncRNAs heat map in the high and low risk group. The asterisks represent the *p* value (*P<0.05; **P<0.01; ***P<0.001).

area under the ROC curve (AUC) for 1, 3, and 5 years also confirmed the good predictive performance of the model where the values of AUC at 1, 3, and 5 years were 0.666, 0.621 and 0.669, respectively. Furthermore, in the ROC curve containing risk score, age, gender, stage, and grade, the AUC value of the risk score was higher than that of other clinical data in predicting the survival of colon cancer patients. The comparison of progression-free survival (PFS) in the high- and low-risk groups was statistically significant. When risk score, age and tumor stages were included in univariate and multivariate Cox regression analyses, they all were inversely proportional to length of survival, and all were independent prognostic factors. Therefore, this model achieved at least comparable accuracy in predicting prognosis from clinical features (**Figure 3**).

Nomogram development and validation for colon cancer

The C-index and calibration plots of the nomogram showed good consistency in predicting survival of colon cancer patients, tumor staging, and risk score. We observed that the 1-year survival probability of patients with a compre-

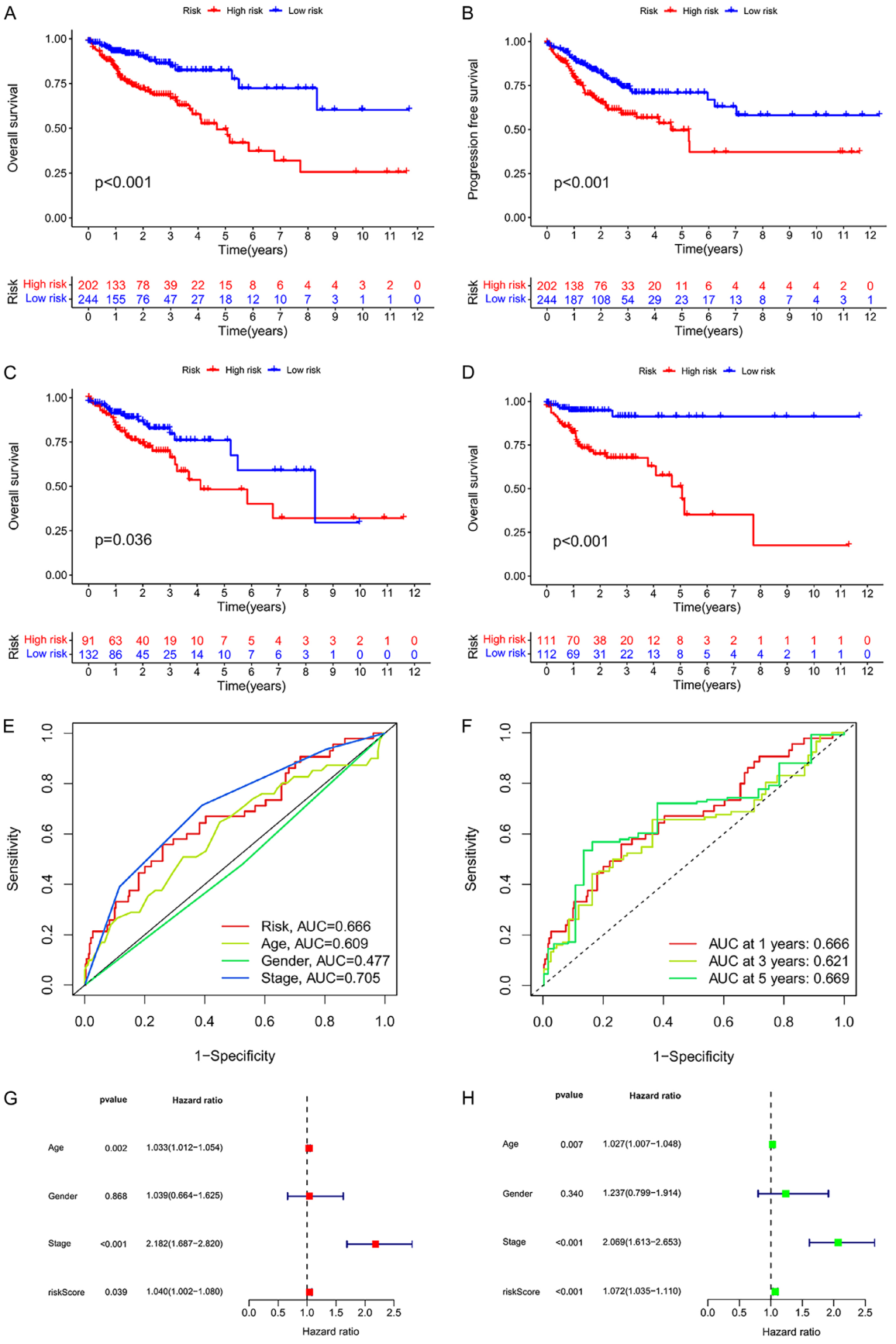
A
Risk High risk Low risk
Overall survival
p<0.001
Time(years)
Risk High risk 202 133 78 39 22 15 8 6 4 4 3 2 0
Low risk 244 155 76 47 27 18 12 10 7 3 1 1 0
B
Risk High risk Low risk
Progression free survival
p<0.001
Time(years)
Risk High risk 202 138 76 33 20 11 6 4 4 4 4 2 0
Low risk 244 187 108 54 29 23 17 13 8 7 4 3 1
C
Risk High risk Low risk
Overall survival
p=0.036
Time(years)
Risk High risk 91 63 40 19 10 7 5 4 3 3 2 1 0
Low risk 132 86 45 25 14 10 7 6 3 1 0 0 0
D
Risk High risk Low risk
Overall survival
p<0.001
Time(years)
Risk High risk 111 70 38 20 12 8 3 2 1 1 1 1 0
Low risk 112 69 31 22 13 8 5 4 4 2 1 1 0
E
Sensitivity
1−Specificity
Risk, AUC=0.666
Age, AUC=0.609
Gender, AUC=0.477
Stage, AUC=0.705
F
Sensitivity
1−Specificity
AUC at 1 years: 0.666
AUC at 3 years: 0.621
AUC at 5 years: 0.669
G
pvalue Hazard ratio
Age 0.002 1.033(1.012−1.054)
Gender 0.868 1.039(0.664−1.625)
Stage <0.001 2.182(1.687−2.820)
riskScore 0.039 1.040(1.002−1.080)
Hazard ratio
H
pvalue Hazard ratio
Age 0.007 1.027(1.007−1.048)
Gender 0.340 1.237(0.799−1.914)
Stage <0.001 2.069(1.613−2.653)
riskScore <0.001 1.072(1.035−1.110)
Hazard ratio

Figure 3. Prognostic value of the risk prediction model in the training, test, and entire sets: (A-D) Kaplan-Meier survival curves of survival probability of patients and PFS between low-and high-risk groups in the training, test, and entire sets, respectively, (E, F) ROC curves to predict the sensitivity and specificity of 1-, 3-, and 5-year survival according to the CRG_score in the training, test, and entire sets, respectively, (G, H) Univariate and multivariate regression analysis of clinical factors (age, gender, risk score, tumor stage) and risk score with OS.

hensive score of 174 in age, gender, risk score, and tumor stage was 0.847. The survival probability for > 3 years was 0.691 whereas the survival probability for > 5 years was 0.552. Concordant with the nomogram results, the 1-, 3-, and 5-year survival calibration curves of the prediction model were plotted. This showed that our predictive model had a high accuracy for the survival for colon cancer patients. We also performed model validation for clinical grouping. The OS of the high- and low-risk groups of stages I-II, and III-IV patients were found, showing that the high-risk group had a shorter OS in comparison to the low-risk group. The risk model could accurately discern and predict survival for patients with early or advanced colon cancer (**Figure 4**).

GO and KEGG enrichment analysis between risk groups

We performed Gene Ontology (GO) enrichment analysis to investigate the role of Cuproptosis-Related lncRNAs in colon cancer. Our results showed that gene sets related to cuproptosis and immunity were significantly enriched in the low-risk group, including categories such as immunoglobulin complex, immunoglobulin production, and antigen binding. KEGG enrichment analysis identified several significant pathways, including vascular smooth muscle contraction, focal adhesion, ECM-receptor interaction, malaria, renin secretion, CGMP-PKG signaling pathway, bile secretion, pancreatic secretion, protein digestion and absorption, and fat digestion and absorption. KEGG pathway annotation revealed that differentially expressed genes (DEGs) were significantly enriched in all 10 pathways, including the ECM-receptor interaction, protein digestion and absorption, and CGMP-PKG signaling pathways. This suggests that additional DEGs and signaling pathways are involved in colon cancer progression. The ECM receptor interaction and focal adhesion pathways have been shown to play a critical role in tumor shedding, adhesion, degradation, movement, and proliferation [26]. Studies have demonstrated that the ECM receptor interaction pathway contributes to the invasion and metastasis of gastric cancer [27], and in colorectal cancer, it promotes epithelial-mesenchymal transition (EMT) [28]. Furthermore, during tumor metastasis, tumor cells utilize ECM receptor interaction pathways, and the tumor suppressor protein Nischarin may interact with multiple proteins to inhibit cancer cell migration [29, 30]. Although invasion and metastasis are a hallmarks of malignant tumors, our results suggest that the expression of ECM receptor interaction pathways in colon cancer tissues may offer new insight for targeted cancer therapy (**Figure 5**).

Comparison of immune microenvironment and drug sensitivity for risk groups

We identified a set of TME-related genes that could predict disease outcome and treatment response of patients with colon cancer. According to the mutation burden correlation analysis, 219 of 228 colon cancer patients in the low-risk group had mutations, and 177 of 186 colon cancer patients in the high-risk group had mutations, mainly related to APC, TP53, TTN, KRAS and PIK3CA genes. The mutation rate was 96.05% in the low-risk group and 95.16% in the high-risk group, respectively.

This study explored the immune microenvironment and drug susceptibility analyses in order to investigate the expression of immunotherapy-related genes and the differences in IC_{50} of therapeutic agents in colon cancer patients. Through copper-death co-expression of lncRNA-related genes, we found that GLS, GCSH, MTF1, ATP7A, and DBT genes were positively correlated. Immune cell infiltration of TCGA primary tumors were downloaded from TIMER web server (https://cistrome.shinyapps.io/timer/) [25]. The infiltration estimation results generated by the TIMER algorithm consist of 6 specific immune cell subsets, including B cells, CD8+ T cells, CD4+ T cells, macrophages, neutrophils, and dendritic cells. We extracted infiltration estimates to assess the relationship between five cuproptosis gene expression levels and dif-

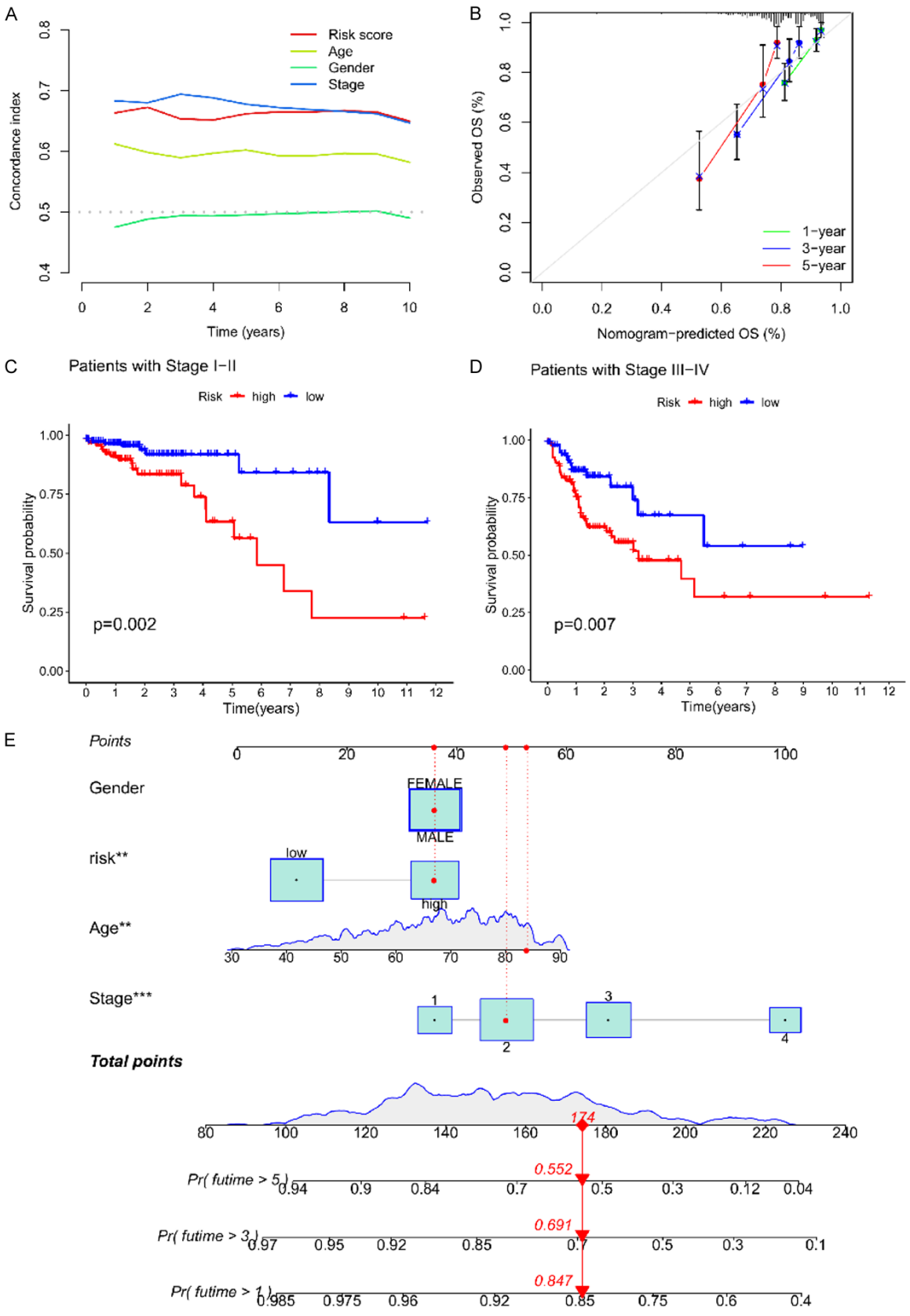

Figure 4. Construction and evaluation of nomogram based on CRG_score: (A) The c-index curve of the model, (B) Calibration curves of the nomogram, (C, D) the OS of the high and low risk groups of stage I-II and III-IV patients respectively, (E) Nomogram for predicting the 1-, 3-, and 5-year OS of colon cancer patients.

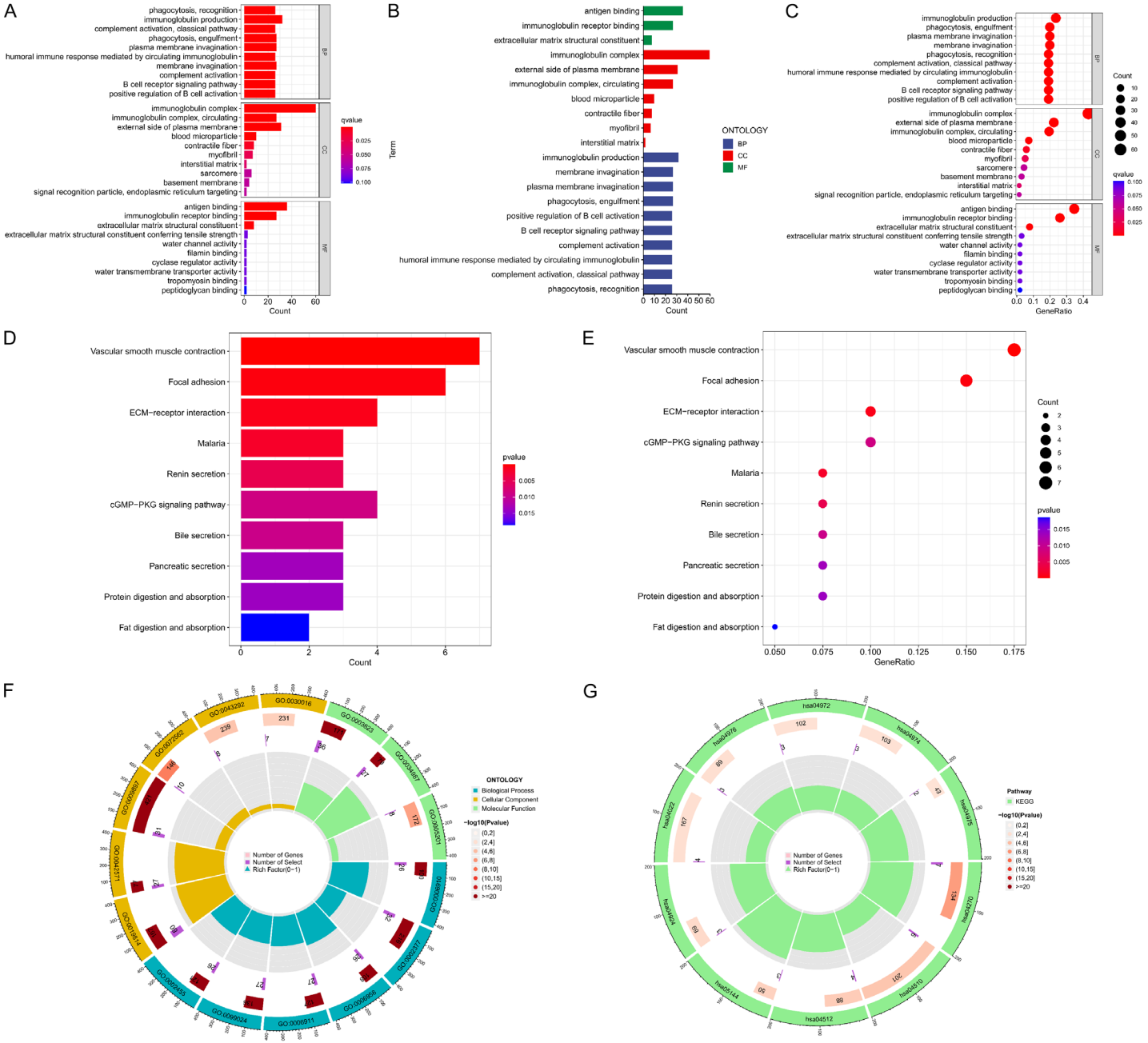
A
phagocytosis, recognition
immunoglobulin production
complement activation, classical pathway
phagocytosis, engulfment
plasma membrane invagination
humoral immune response mediated by circulating immunoglobulin
membrane invagination
complement activation
B cell receptor signaling pathway
positive regulation of B cell activation
immunoglobulin complex
immunoglobulin complex, circulating
external side of plasma membrane
blood microparticle
contractile fiber
myofibril
interstitial matrix
sarcomere
basement membrane
signal recognition particle, endoplasmic reticulum targeting
antigen binding
immunoglobulin receptor binding
extracellular matrix structural constituent
extracellular matrix structural constituent conferring tensile strength
water channel activity
filamin binding
cyclase regulator activity
water transmembrane transporter activity
tropomyosin binding
peptidoglycan binding
BP
CC
MF
qvalue
Count
B
antigen binding
immunoglobulin receptor binding
extracellular matrix structural constituent
immunoglobulin complex
external side of plasma membrane
immunoglobulin complex, circulating
blood microparticle
contractile fiber
myofibril
interstitial matrix
immunoglobulin production
membrane invagination
plasma membrane invagination
phagocytosis, engulfment
positive regulation of B cell activation
B cell receptor signaling pathway
complement activation
humoral immune response mediated by circulating immunoglobulin
complement activation, classical pathway
phagocytosis, recognition
Term
Count
ONTOLOGY
BP
CC
MF
C
immunoglobulin production
phagocytosis, engulfment
plasma membrane invagination
membrane invagination
phagocytosis, recognition
complement activation, classical pathway
humoral immune response mediated by circulating immunoglobulin
complement activation
B cell receptor signaling pathway
positive regulation of B cell activation
immunoglobulin complex
external side of plasma membrane
immunoglobulin complex, circulating
blood microparticle
contractile fiber
myofibril
sarcomere
basement membrane
interstitial matrix
signal recognition particle, endoplasmic reticulum targeting
antigen binding
immunoglobulin receptor binding
extracellular matrix structural constituent
extracellular matrix structural constituent conferring tensile strength
water channel activity
filamin binding
cyclase regulator activity
water transmembrane transporter activity
tropomyosin binding
peptidoglycan binding
Count
qvalue
GeneRatio
D
Vascular smooth muscle contraction
Focal adhesion
ECM−receptor interaction
Malaria
Renin secretion
cGMP−PKG signaling pathway
Bile secretion
Pancreatic secretion
Protein digestion and absorption
Fat digestion and absorption
Count
pvalue
E
Vascular smooth muscle contraction
Focal adhesion
ECM−receptor interaction
cGMP−PKG signaling pathway
Malaria
Renin secretion
Bile secretion
Pancreatic secretion
Protein digestion and absorption
Fat digestion and absorption
GeneRatio
Count
pvalue
F
Number of Genes
Number of Select
Rich Factor(0−1)
ONTOLOGY
Biological Process
Cellular Component
Molecular Function
−log10(Pvalue)
G
hsa04972
hsa04974
hsa04976
hsa04975
hsa04970
hsa04510
hsa04512
hsa04514
hsa04024
hsa04022
Number of Genes
Number of Select
Rich Factor(0−1)
Pathway
KEGG
−log10(Pvalue)

Figure 5. Pathway enrichment analysis of CRGs in colon cancer patients in the TCGA: (A-C, F) the enriched item in the gene ontology analysis, (D, E, G) the enriched item in the Kyoto Encyclopedia of Genes and Genomes analysis.

ferent immune cell subsets in colorectal cancer. These were analyzed using TIMER, with $P<0.05$ considered significant. We found that GLS, MTF1, ATP7A, and DBT genes were associated with colon cancer immune B cells. CD8+ T cell, CD4+ T cell, macrophage, neutrophil, and dendritic cell secretion were positively correlated, suggesting that copper death-related lncRNA may play an important role in regulation of the colon cancer immune microenvironment. We found that the expression of MTF1 gene was highly correlated with CD8+ T cell, CD4+ T cell, neutrophil, and dendritic cell development (correlation coefficients were 0.42, 0.506, 0.551, and 0.558 where $P<0.05$ was considered significant). The expression of ATP7A was correlated with the secretion of CD4+ T cell (correlation coefficient was 0.412, $P<0.05$).

Furthermore, the expressions of B cells, neutrophils, and DC cells were significantly different in the high and low risk groups. The correlations between B cells and T CD4 cells, DC cells, and T CD8 cells were all significant. We further analyzed the relationship between immune cells and survival and found that the expression of B cells was statistically different in the high and low risk groups, where it was better in the high risk group than the low risk group. However, macrophages were statistically significant for the high and low risk groups, and the survival of the high risk group was worse than that of the low risk group. At the immune checkpoint, we found that the expression of CTLA4, CD274, and TIGIT were significantly different between the two groups.

By analyzing drug sensitivity, we found that in the low-risk group, the IC_{50} of CAL-101, QL-XII-47, CGP-082996, DMOG, Rapamycin, Salubrinal, Sunitinib, TGX221, WZ-1-84, XL-184, and ZSTK474 were lower than those of the high-risk group. Our results showed that the IC_{50} value of the high-risk group was lower than that of the low-risk group and the two groups differed significantly (**Figures 6**-**9**).

Discussion

Bioinformatics has enabled significant strides, particularly in database development and the application of deep learning methods, advancing our understanding of cancer mechanisms [31, 32]. The role of copper in cellular processes such as energy metabolism, ROS detoxification, and signaling is essential. As previously established, elevated cellular copper levels can bind to TCA cycle components, inducing mitochondrial dysfunction and eventually leading to cell death [12]. This process, known as cuproptosis, has crucial antiangiogenic effects in tumor cells. Studies have shown that copper-induced ROS, including superoxide anions, hydroxyl radicals, and hydrogen peroxide, contribute to tumorigenesis and cell death. Copper's therapeutic potential is evident in fields like chemodynamic therapy, chemotherapy, and phototherapy [14].

Our study highlights the significant role of cuproptosis-related genes (CRGs) in colorectal cancer (CRC). Functional analysis revealed that TCA cycle-related pathways were abundant, corroborating previous findings that copper dysregulation affects CRC development and progression. Notably, ATP7A, a copper transport ATPase, was found to influence tumor immunity and prognosis by modulating the tumor microenvironment and immune cell infiltration [33, 34]. This aligns with studies showing that ATP7A affects VEGFR2 signaling and angiogenesis by inhibiting autophagy-mediated degradation of VEGFR2 [35]. Previous research has linked ATP7A to a poor prognosis in CRC, and our findings suggest that high ATP7A expression could be a biomarker for immunotherapy response, particularly anti-PD-1/PD-L1 treatments. Increasing evidence underscores the importance of cuproptosis in the tumor immune microenvironment (TME). Recent studies have also explored the prognostic value of cuproptosis-related lncRNAs, supporting the idea that these molecules may be biomarkers for CRC prognosis. Our analysis of 13 cuproptosis-related lncRNAs revealed differential expression between tumor and normal tissues, which was strongly associated with overall survival (OS) and progression-free survival (PFS), further confirming their clinical relevance. In terms of ECM, our findings are consistent with reports suggesting that ECM components provide structural support and regulate tumor progression through mechanical and signaling

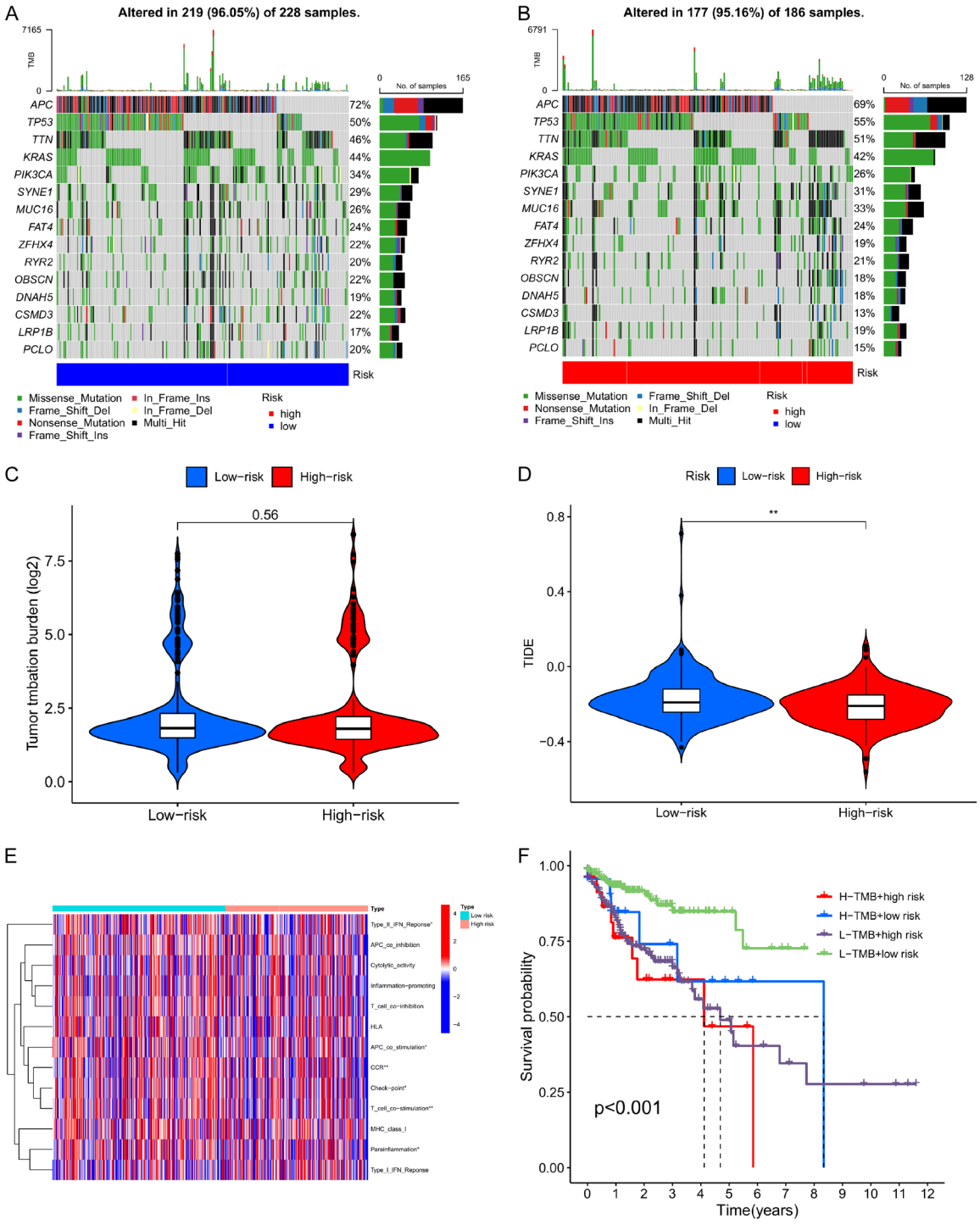

Figure 6. Genetic characteristics of CRG_score and tumor somatic mutation of colon cancer: (A, B) Waterfall plot of tumor somatic mutation established by those with low- and high-risk group, (C) Tumor mutation burden in high- and low-risk groups, (D) Tumor Immune Dysfunction and Exclusion (TIDE) score in colon cancer, (E) Immune heat map of Cuproptosis-Related lncRNAs, in colon cancer in high and low risk groups, (F) Overall survival of the patients stratified by both the CRG-score signature and TMB using Kaplan-Meier curves.

pathways. The interaction between cancer cells and ECM components, leading to mechanical transduction abnormalities, plays a crucial role in malignant transformation [36]. We also

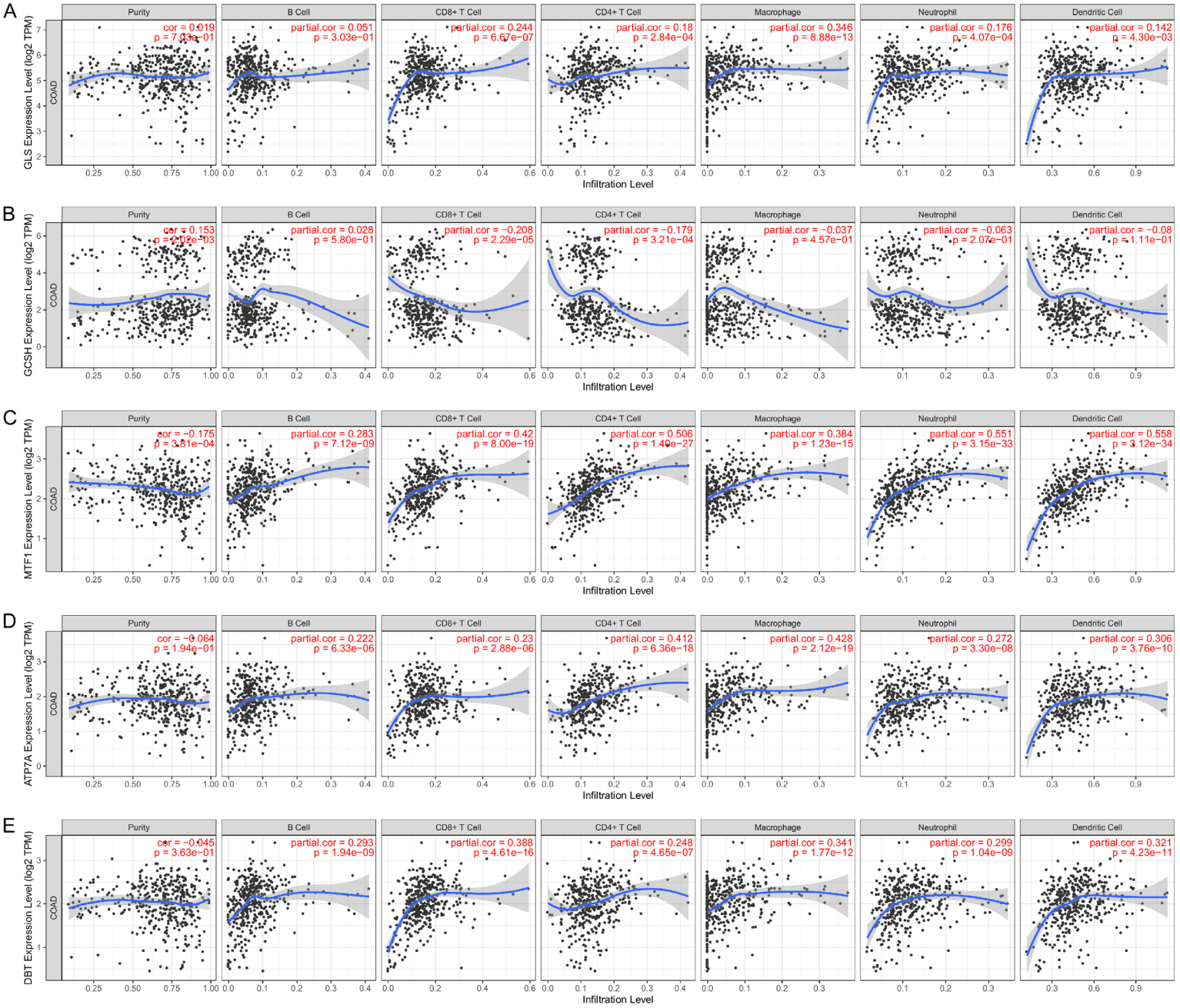
A
B
C
D
E
Purity
B Cell
CD8+ T Cell
CD4+ T Cell
Macrophage
Neutrophil
Dendritic Cell
COAD
GLS Expression Level (log2 TPM)
GCSH Expression Level (log2 TPM)
MTF1 Expression Level (log2 TPM)
ATP7A Expression Level (log2 TPM)
DBT Expression Level (log2 TPM)
Infiltration Level
cor = 0.019
p = 7.03e−01
partial.cor = 0.051
p = 3.03e−01
partial.cor = 0.244
p = 6.67e−07
partial.cor = 0.18
p = 2.84e−04
partial.cor = 0.346
p = 8.88e−13
partial.cor = 0.176
p = 4.07e−04
partial.cor = 0.142
p = 4.30e−03
cor = 0.153
p = 2.02e−03
partial.cor = 0.028
p = 5.80e−01
partial.cor = −0.208
p = 2.29e−05
partial.cor = −0.179
p = 3.21e−04
partial.cor = −0.037
p = 4.57e−01
partial.cor = −0.063
p = 2.07e−01
partial.cor = −0.08
p = 1.11e−01
cor = −0.175
p = 3.81e−04
partial.cor = 0.283
p = 7.12e−09
partial.cor = 0.42
p = 8.00e−19
partial.cor = 0.506
p = 1.40e−27
partial.cor = 0.384
p = 1.23e−15
partial.cor = 0.551
p = 3.15e−33
partial.cor = 0.558
p = 3.12e−34
cor = −0.064
p = 1.94e−01
partial.cor = 0.222
p = 6.33e−06
partial.cor = 0.23
p = 2.88e−06
partial.cor = 0.412
p = 6.36e−18
partial.cor = 0.428
p = 2.12e−19
partial.cor = 0.272
p = 3.30e−08
partial.cor = 0.306
p = 3.76e−10
cor = −0.045
p = 3.63e−01
partial.cor = 0.293
p = 1.94e−09
partial.cor = 0.388
p = 4.61e−16
partial.cor = 0.248
p = 4.65e−07
partial.cor = 0.341
p = 1.77e−12
partial.cor = 0.299
p = 1.04e−09
partial.cor = 0.321
p = 4.23e−11

Figure 7. Correlation between (A) GLS, (B) GCSH, (C) MTF1, (D) ATP7A and (E) DBT expression and immune infiltration in colon cancer in the TIMER database.

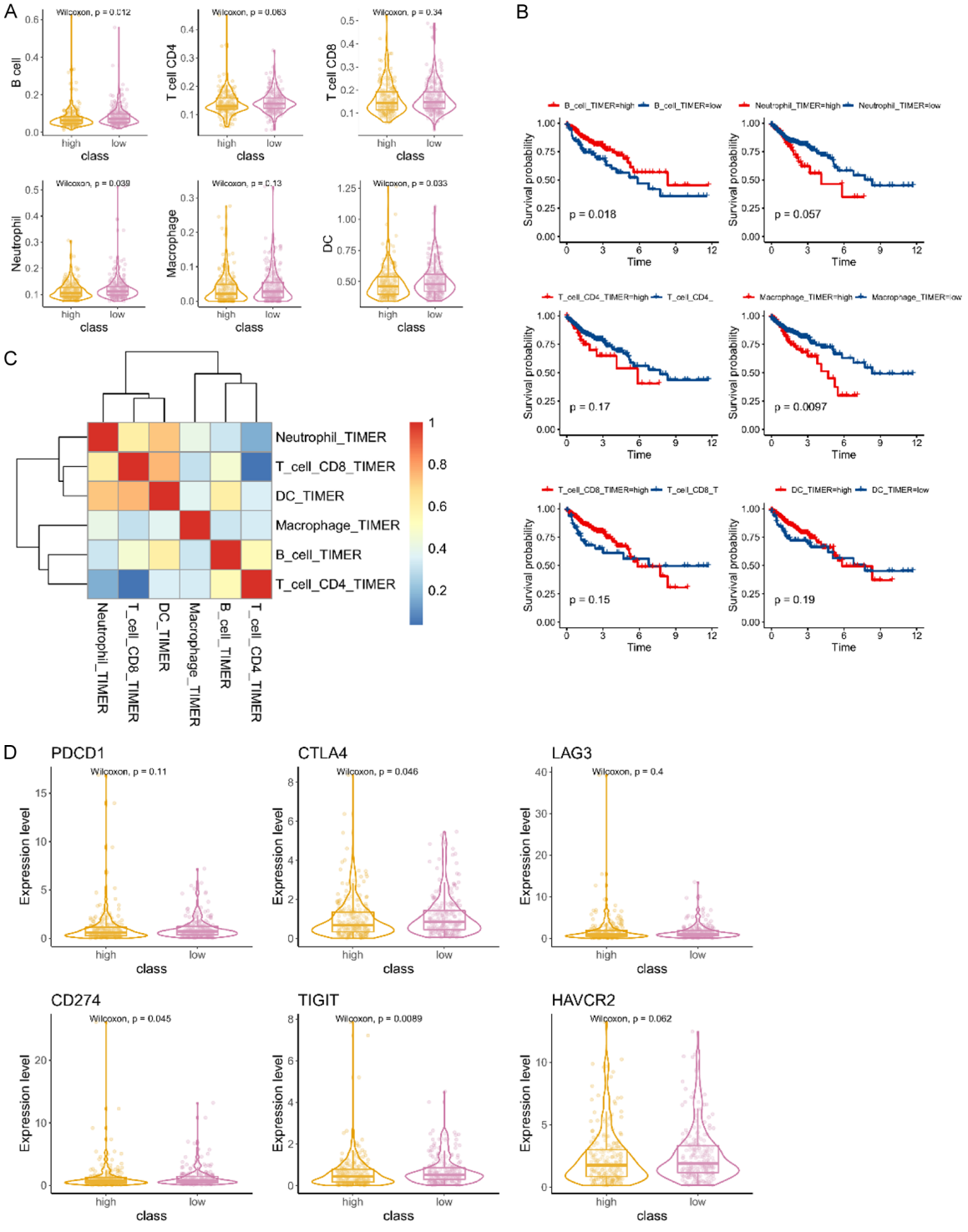

Figure 8. Immune environment and prognosis: (A) Differential expression of immune cells, (B) Relationship between immune cells and prognosis, (C) Correlation between immune cells, (D) Differences in immune checkpoint expression.

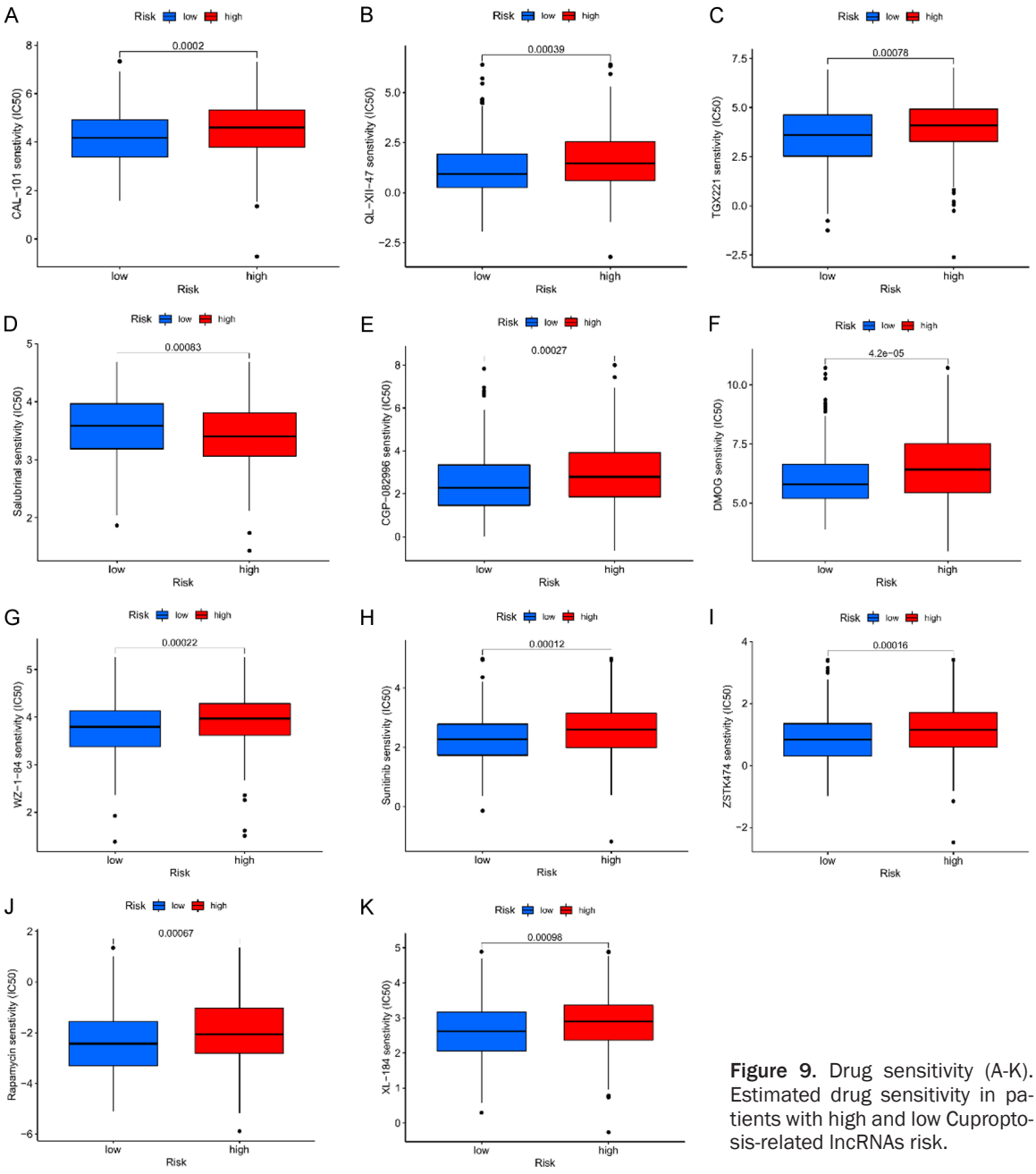

Figure 9. Drug sensitivity (A-K). Estimated drug sensitivity in patients with high and low Cuproptosis-related lncRNAs risk.

found that ECM normalization, coupled with treatments such as nanoparticles containing piperidine and NLG919, can enhance the efficacy of chemotherapy and immunotherapy, which is consistent with studies indicating that ECM remodeling can improve therapeutic outcomes [37].

Our prognostic model based on cuproptosis-related lncRNAs was able to stratify CRC patients into high- and low-risk groups, with survival analysis revealing significantly better OS in the low-risk group. These results align with previous research linking risk scores to prognosis in CRC. The model also demonstrated strong predictive performance, similar to other models based on molecular signatures. Our use of Cox regression and Lasso regression, combined with elastic net regularization, resulted in a robust model for predicting patient prognosis. The association of the 7 lncRNAs (including EIF1AX-AS1, MCCC1-AS1, and ALMS1-IT1) with tumor development or prognosis in CRC supports earlier studies that

identified these lncRNAs as key players in cancer progression [38, 39]. Additionally, univariate and multivariate Cox regression analysis confirmed the independent predictive value of the risk score and tumor stage, which is in line with findings from other studies that emphasize the importance of staging in CRC prognosis. The model's accuracy in predicting 1-, 3-, and 5-year OS further corroborates its potential for clinical application, as seen in similar models that use molecular signatures for personalized cancer treatment. Finally, we constructed a prognostic nomogram based on cuproptosis-related lncRNAs, incorporating age and tumor stage as independent risk factors. Our model's ability to predict accurately the OS across various time points aligns with current trends in precision medicine, underscoring the importance of individualized treatment strategies based on molecular markers.

In this study, we utilized LASSO Cox regression to identify prognostic factors, including tumor stage and cuproptosis-related lncRNAs risk score, both of which were statistically significant. These findings are consistent with prior research linking tumor stage to prognosis in colorectal cancer (CRC) [40, 41]. Kaplan-Meier survival analysis demonstrated better overall survival (OS) and progression-free survival (PFS) in the low-risk group, which aligns with similar studies that show cuproptosis-related factors correlate with better prognosis in cancer [42]. Moreover, somatic mutation analysis revealed that higher risk scores were associated with mutations in key oncogenes such as APC, TP53, and KRAS. This concurs with existing literature on the elevated mutation rates of these genes in colon cancer. Our TIMER algorithm analysis revealed that cuproptosis-related genes (CRGs) significantly correlated with immune cell infiltration, particularly B cells, CD8+ T cells, and macrophages. These results support findings from other studies showing that immune cell interactions, particularly macrophages, play a pivotal role in tumor progression [43, 44]. Our data also showed significant differences in immune cell expression between the high- and low-risk groups, with B cells linked to improved outcome and macrophages associated with worse outcome. These findings are in line with previous reports that highlight the dual roles of immune cells, with B cells promoting anti-tumor immunity and macrophages contributing to malignancy. Additionally, we observed notable variations in immune checkpoint markers (CTLA4, CD274, TIGIT), suggesting potential differences in immunotherapy efficacy, a point supported by recent studies indicating the role of these markers for immune evasion in cancer. The present study strengthens the case for using cuproptosis gene risk scores as an independent prognostic biomarker for CRC, a conclusion that aligns with the growing body of research supporting the clinical relevance of metabolic pathways in cancer. While TCGA-COAD data were utilized for this cohort study, further experimental validation using qRT-PCR, cell-based assays, and animal models is warranted. GSEA results and *in vitro/in vivo* studies will provide deeper insights into the molecular mechanisms of these lncRNAs and their effect on the tumor microenvironment.

Conclusion

This study conducted a comprehensive analysis of cuproptosis-related genes (CRGs) in colon cancer, exploring their functional and immune status, and established a predictive model based on CRGs to assess the prognosis of colon cancer patients. The research provides a novel methodological framework for studying immune-related colon cancer from the perspective of cuproptosis-related genes, tumor microenvironment (TME), and emerging biomarkers for immunotherapy.

Acknowledgements

The authors would like to express their gratitude to EditSprings (https://www.editsprings.cn) for the expert linguistic services provided. This project was supported by the Guangxi Medical and Health Key Cultivation Discipline Construction Project (2021063).

Disclosure of conflict of interest

None.

Abbreviations

CRGs, Cuproptosis-related genes; TME, Tumor microenvironment; TIME, Tumor immune microenvironment; TCA, Tricarboxylic acid; OS, Overall survival; ROC, Receiver operating characteristic; TMB, Tumor mutation burden; MF, Molecular function; BP, Biological pathways; CC, Cellular components.

Address correspondence to: Bo Zhao, Department of General Surgery, The Second Affiliated Hospital of Guangxi Medical University, No. 166, East University Road, Xixiangtang District, Nanning 530021, Guangxi Zhuang Autonomous Region, The People's Republic of China. E-mail: 1118zhaobo@163.com

References

[1] Phipps O, Brookes MJ and Al-Hassi HO. Iron deficiency, immunology, and colorectal cancer. Nutr Rev 2021; 79: 88-97.
[2] Vitale I, Manic G, Coussens LM, Kroemer G and Galluzzi L. Macrophages and metabolism in the tumor microenvironment. Cell Metab 2019; 30: 36-50.
[3] Anderson NM and Simon MC. The tumor microenvironment. Curr Biol 2020; 30: R921-R925.
[4] Hinshaw DC and Shevde LA. The tumor microenvironment innately modulates cancer progression. Cancer Res 2019; 79: 4557-4566.
[5] Maus MV and June CH. Making better chimeric antigen receptors for adoptive T-cell therapy. Clin Cancer Res 2016; 22: 1875-1884.
[6] Zhang Y, Song J, Zhao Z, Yang M, Chen M, Liu C, Ji J and Zhu D. Single-cell transcriptome analysis reveals tumor immune microenvironment heterogenicity and granulocytes enrichment in colorectal cancer liver metastases. Cancer Lett 2020; 470: 84-94.
[7] Lin A, Zhang J and Luo P. Crosstalk between the MSI status and tumor microenvironment in colorectal cancer. Front Immunol 2020; 11: 2039.
[8] Chen J, Jiang Y, Shi H, Peng Y, Fan X and Li C. The molecular mechanisms of copper metabolism and its roles in human diseases. Pflugers Arch 2020; 472: 1415-1429.
[9] Kepp KP and Squitti R. Copper imbalance in Alzheimer's disease: convergence of the chemistry and the clinic. Coordination Chemistry Reviews 2019; 397: 168-187.
[10] Sacco A, Martelli F, Pal A, Saraceno C, Benussi L, Ghidoni R, Rongioletti M and Squitti R. Regulatory miRNAs in cardiovascular and Alzheimer's disease: a focus on copper. Int J Mol Sci 2022; 23: 3327.
[11] Khoshdel Z, Naghibalhossaini F, Abdollahi K, Shojaei S, Moradi M and Malekzadeh M. Serum copper and zinc levels among Iranian colorectal cancer patients. Biol Trace Elem Res 2016; 170: 294-299.
[12] Kahlson MA and Dixon SJ. Copper-induced cell death. Science 2022; 375: 1231-1232.
[13] Saporito-Magriñá CM, Musacco-Sebio RN, Andrieux G, Kook L, Orrego MT, Tuttolomondo MV, Desimone MF, Boerries M, Borner C and Repetto MG. Copper-induced cell death and the protective role of glutathione: the implication of impaired protein folding rather than oxidative stress. Metallomics 2018; 10: 1743-1754.
[14] Jiang Y, Huo Z, Qi X, Zuo T and Wu Z. Copper-induced tumor cell death mechanisms and antitumor theragnostic applications of copper complexes. Nanomedicine (Lond) 2022; 17: 303-324.
[15] Bhan A, Soleimani M and Mandal SS. Long noncoding RNA and cancer: a new paradigm. Cancer Res 2017; 77: 3965-3981.
[16] Tan YT, Lin JF, Li T, Li JJ, Xu RH and Ju HQ. LncRNA-mediated posttranslational modifications and reprogramming of energy metabolism in cancer. Cancer Commun (Lond) 2021; 41: 109-120.
[17] Yang L, Yu J, Tao L, Huang H, Gao Y, Yao J and Liu Z. Cuproptosis-related lncRNAs are biomarkers of prognosis and immune microenvironment in head and neck squamous cell carcinoma. Front Genet 2022; 13: 947551.
[18] Zhou Y, Shu Q, Fu Z, Wang C, Gu J, Li J, Chen Y and Xie M. A novel risk model based on cuproptosis-related lncRNAs predicted prognosis and indicated immune microenvironment landscape of patients with cutaneous melanoma. Front Genet 2022; 13: 959456.
[19] Li X, Zhou W, Zhu C, Liu J, Ming Z, Ma C and Li Q. Multi-omics analysis reveals prognostic and therapeutic value of cuproptosis-related lncRNAs in oral squamous cell carcinoma. Front Genet 2022; 13: 984911.
[20] Goldman MJ, Craft B, Hastie M, Repečka K, McDade F, Kamath A, Banerjee A, Luo Y, Rogers D, Brooks AN, Zhu J and Haussler D. Visualizing and interpreting cancer genomics data via the Xena platform. Nat Biotechnol 2020; 38: 675-678.
[21] Cibulskis K, Lawrence MS, Carter SL, Sivachenko A, Jaffe D, Sougnez C, Gabriel S, Meyerson M, Lander ES and Getz G. Sensitive detection of somatic point mutations in impure and heterogeneous cancer samples. Nat Biotechnol 2013; 31: 213-219.
[22] Mayakonda A, Lin DC, Assenov Y, Plass C and Koeffler HP. Maftools: efficient and comprehensive analysis of somatic variants in cancer. Genome Res 2018; 28: 1747-1756.
[23] Franz M, Rodriguez H, Lopes C, Zuberi K, Montojo J, Bader GD and Morris Q. GeneMANIA update 2018. Nucleic Acids Res 2018; 46: W60-W64.
[24] Yu G, Wang LG, Han Y and He QY. clusterProfiler: an R package for comparing biological themes among gene clusters. OMICS 2012; 16: 284-287.
[25] Li T, Fan J, Wang B, Traugh N, Chen Q, Liu JS, Li B and Liu XS. TIMER: a web server for compre-

hensive analysis of tumor-infiltrating immune cells. Cancer Res 2017; 77: e108-e110.
[26] Sa S, Wong L and McCloskey KE. Combinatorial fibronectin and laminin signaling promote highly efficient cardiac differentiation of human embryonic stem cells. Biores Open Access 2014; 3: 150-161.
[27] Yan P, He Y, Xie K, Kong S and Zhao W. In silico analyses for potential key genes associated with gastric cancer. PeerJ 2018; 6: e6092.
[28] Chen QK, Lee K, Radisky DC and Nelson CM. Extracellular matrix proteins regulate epithelial-mesenchymal transition in mammary epithelial cells. Differentiation 2013; 86: 126-132.
[29] Alahari SK. Nischarin inhibits Rac induced migration and invasion of epithelial cells by affecting signaling cascades involving PAK. Exp Cell Res 2003; 288: 415-424.
[30] Bao Y, Wang L, Shi L, Yun F, Liu X, Chen Y, Chen C, Ren Y and Jia Y. Transcriptome profiling revealed multiple genes and ECM-receptor interaction pathways that may be associated with breast cancer. Cell Mol Biol Lett 2019; 24: 38.
[31] Sohail A and Arif F. Supervised and unsupervised algorithms for bioinformatics and data science. Prog Biophys Mol Biol 2020; 151: 14-22.
[32] Subramanian I, Verma S, Kumar S, Jere A and Anamika K. Multi-omics data integration, interpretation, and its application. Bioinform Biol Insights 2020; 14: 1177932219899051.
[33] Li YQ, Yin JY, Liu ZQ and Li XP. Copper efflux transporters ATP7A and ATP7B: Novel biomarkers for platinum drug resistance and targets for therapy. IUBMB Life 2018; 70: 183-191.
[34] Petruzzelli R and Polishchuk RS. Activity and trafficking of copper-transporting ATPases in tumor development and defense against platinum-based drugs. Cells 2019; 8: 1080.
[35] Ash D, Sudhahar V, Youn SW, Okur MN, Das A, O'Bryan JP, McMenamin M, Hou Y, Kaplan JH and Fukai T. The P-type ATPase transporter ATP7A promotes angiogenesis by limiting autophagic degradation of VEGFR2. Nat Commun 2021; 12: 3091.
[36] Huang J, Zhang L, Wan D, Zhou L, Zheng S, Lin S and Qiao Y. Extracellular matrix and its therapeutic potential for cancer treatment. Signal Transduct Target Ther 2021; 6: 153.
[37] Hou B, Zhou L, Wang H, Saeed M, Wang D, Xu Z, Li Y and Yu H. Engineering stimuli-activatable boolean logic prodrug nanoparticles for combination cancer immunotherapy. Adv Mater 2020; 32: e1907210.
[38] Lv C, Sun J, Ye Y, Lin Z, Li H, Liu Y, Mo K, Xu W, Hu W, Draz E and Wang S. Long noncoding RNA EIF1AX-AS1 promotes endometrial cancer cell apoptosis by affecting EIF1AX mRNA stabilization. Cancer Sci 2022; 113: 1277-1291.
[39] Mei J, Cao G, He H, Chang J, Zhang B and Mei Y. Effects of long non-coding RNA ALMS1-IT1 on the proliferation and migration of colorectal cancer cells via regulating the expressions of miRNA-889-3p and ATAD2. Cancer Research and Clinic 2021; 818-823.
[40] Dolatkhah R, Somi MH, Shabanloei R, Farassati F, Fakhari A and Dastgiri S. Main risk factors association with proto-oncogene mutations in colorectal cancer. Asian Pac J Cancer Prev 2018; 19: 2183-2190.
[41] Ades S, Kumar S, Alam M, Goodwin A, Weckstein D, Dugan M, Ashikaga T, Evans M, Verschraegen C and Holmes CE. Tumor oncogene (KRAS) status and risk of venous thrombosis in patients with metastatic colorectal cancer. J Thromb Haemost 2015; 13: 998-1003.
[42] Wang JJ, Siu MK, Jiang YX, Leung TH, Chan DW, Wang HG, Ngan HY and Chan KK. A combination of glutaminase inhibitor 968 and PD-L1 blockade boosts the immune response against ovarian cancer. Biomolecules 2021; 11: 1749.
[43] Mehla K and Singh PK. Metabolic regulation of macrophage polarization in cancer. Trends Cancer 2019; 5: 822-834.
[44] Anderson NR, Minutolo NG, Gill S and Klichinsky M. Macrophage-based approaches for cancer immunotherapy. Cancer Res 2021; 81: 1201-1208.